Chapter 1

CMS-EXO-16-010: a CMS search for dark matter in the mono-Z channel (2.3 fb^{-1})

B. Fuks

The results presented in the CMS-EXO-16-010 experimental analysis are interpreted in the framework of several models. This includes a simplified tree-level ultraviolet-complete model for dark matter where a fermionic dark matter particle couples to the Standard Model sector through interactions with a spin-1 mediator [1], an effective dark matter model featuring higher-dimensional four-point interactions of a pair of dark matter particles with two of the Standard Model electroweak gauge bosons [1], and an effective model describing unparticle dynamics [2, 3].

The validation material that has been provided by the CMS collaboration (upon our request) only relies on the first of these three models. In this context, the Standard Model is extended by a dark matter particle χ that is assumed to be a Dirac fermion of mass m_χ whose interactions with the Standard Model quarks are mediated by a spin-1 mediator Z' of mass $m_{Z'}$. The interactions of the Z' boson are moreover imposed to be of a purely vector nature, the corresponding Lagrangian reading thus

$$\begin{aligned}\mathcal{L} = \mathcal{L}_{\rm SM} &- \frac{1}{4} Z'_{\mu\nu} Z'^{\mu\nu} + \frac{1}{2} m^2_{Z'} Z'^{\mu} Z'_{\mu} + i\bar{\chi}\partial\!\!\!/\chi - m\bar{\chi}\chi \\ &- Z'_\mu \left[\sum_{q=u,d} g_q \bar{q}\gamma^\mu q + g_\chi \bar{\chi}\gamma^\mu \chi \right] .\end{aligned} \tag{1.1}$$

The $\mathcal{L}_{\rm SM}$ Lagrangian represents the Standard Model Lagrangian, $Z'_{\mu\nu}$ denotes the field strength tensor of the Z' boson and flavor indices are moreover understood for what concern the new physics interactions of the quarks. The strength of the interaction of the Z' mediator with the dark matter particle is denoted by g_χ, whilst the couplings to the Standard Model quarks are universal and read g_u and g_d for up-type and down-type quarks, respectively. Although interactions with charged leptons and neutrinos are in principle possible, they are ignored for simplicity.

In this theoretical framework, a mono-Z-boson final state could emerge from quark-antiquark annihilation. This is illustrated by the representative Feynman diagram shown in Figure 1.1 in which the Z-boson decay into a leptonic final state is included.

The validation material provided by the CMS collaboration contains five cutflow charts related to benchmark setups in which the dark matter mass and the new physics couplings have been fixed to

$$m_\chi = 50 \text{ GeV} \qquad \text{and} \qquad g_\chi = g_u = g_d = 1 \,, \tag{1.2}$$

and that differ by the choice of the mediator mass,

$$m_{Z'} \in \big[10, 200, 500, 1000, 5000\big] \text{ GeV}. \tag{1.3}$$

For each scenario, CMS has provided official cutflow charts, as well as information on the configuration of the Monte Carlo event generators that have been used to generate the dark matter signal. This material has been made available on the MADANALYSIS 5 Public Analysis Database,
http://madanalysis.irmp.ucl.ac.be/wiki/PublicAnalysisDatabase.

The provided information including Monte Carlo setup files, this prevents us from introducing any bias at the level of the generation of the signal events. Differences at this levelknowing that such a bias

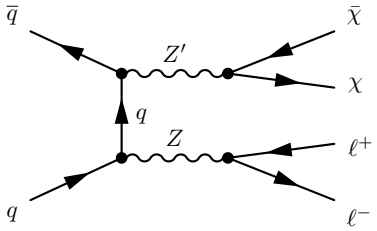

Fig. 1.1: Representative Feynman diagrams for the production of a pair of dark matter particles χ with a leptonically-decaying Z-boson.

could indeed impact, in an uncontroled way, the comparison of the MADANALYSIS 5 results with the CMS results. In addition, our validation procedure includes a comparison of the histograms that have been implemented in the MADANALYSIS 5 code to those shown in the CMS note for the same dark matter model.

The other theoretical contexts in which CMS has interpreted the results have not been addressed in our validation procedure, as precise information on event generation has not been provided. The performed comparisons however make us confident about the reasonable level of accuracy reached by our reimplementation.

Samples of 300.000 simulated dark matter events (including electronic or muonic Z-boson decays) have been generated using MADGRAPH5_aMC@NLO [4] for the simulation of the hard scattering process and PYTHIA 8 [5] for the simulation of the hadronic environment (parton showering and hadronization), using the Monash tune [6]. The hard scattering matrix element associated with the signal process

$$pp \to \left(Z' \to \bar{\chi}\chi\right)\left(Z \to \ell^+\ell^-\right) \tag{1.4}$$

is evaluated at the leading-order accuracy and convoluted with the leading-order set of NNPDF parton densities version 3.0 [7], the latter being accessed via the LHAPDF library [**?**, 8]. The renormalization and factorization scales are moreover set to the geometric mean of the transverse mass of all final-state particles, and the width of the mediator is calculated automatically by means of the MADWIDTH program [9]. In order to evaluate the number of signal events surviving each cut and the number of signal events populating both signal regions, we use the standard recasting methods implemented within MADANALYSIS 5. We begin with a recasting procedure ignoring any pileup effect.

The comparison of the results obtained with MADANALYSIS 5 to the official numbers provided by the CMS collaboration is shown in Table 1.1, Table 1.2, Table 1.3, Table 1.4 and Table 1.5 for a benchmark scenario in which the mediator mass has been fixed to 10 GeV, 200 GeV, 500 GeV, 1000 GeV and 5000 GeV, respectively. For each cut, we present the selection efficiency defined by

$$\epsilon_i = \frac{n_i}{n_{i-1}} \,, \tag{1.5}$$

where n_{i-1} and n_i correspond to the event number before and after the considered cut, respectively. The relative difference between the MADANALYSIS 5 recasting and the CMS official results is normalized to the CMS result, and thus estimated, for each cut, by

$$\delta_i^{\rm rel} = \left| 1 - \frac{\epsilon_i^{\rm MA5}}{\epsilon_i^{\rm CMS}} \right| . \tag{1.6}$$

Results for the firsts selection, i.e.,, the requirement of the presence of two eletrons (in the electron channel) or muons (in the muon channel) are not shown as they have not been provided by the CMS collaboration.

Table 1.1: Comparison of results obtained with our MADANALYSIS 5 reimplementation (MA5) and those provided by the CMS collaboration (CMS) for a dark matter benchmark scenario where the dark matter mass has been set to 50 GeV and the mediator mass to 10 GeV. All vector couplings of the mediator have been fixed to 1. The results are expressed in terms of selection efficiencies as defined in Eq. (1.5), and the relative difference between the CMS and the MADANALYSIS 5 efficiencies, $\delta_i^{\rm rel}$, stems from Eq. (1.6).

	Selection step	Electron channel			Muon channel		
		$\epsilon_i^{\rm CMS}$	$\epsilon_i^{\rm MA5}$	$\delta_i^{\rm rel}$	$\epsilon_i^{\rm CMS}$	$\epsilon_i^{\rm MA5}$	$\delta_i^{\rm rel}$
1	Two leptons	-	-	-	-	-	-
2	$m_{\ell\ell} \in [80, 100]$ GeV	0.929	0.933	0.4%	0.919	0.933	1.5%
3	$p_T^{\ell\ell} > 50$ GeV	0.647	0.648	0.2%	0.644	0.638	1.0%
4	Third lepton and tau veto	0.963	0.992	3.0%	0.961	0.991	3.2%
5	b-jet veto	0.983	0.933	5.1%	0.984	0.931	5.4%
6	$\left\|\Delta\varphi(\not{\mathbf{p}}_T, \mathbf{p}^{\ell\ell})\right\| > 2.7$	0.694	0.761	9.6%	0.705	0.762	8.0%
7	$\left\|\not{E}_T - p_T^{\ell\ell}\right\|/p_T^{\ell\ell} < 0.2$	0.623	0.715	15.0%	0.623	0.704	13.0%
8	$\not{E}_T > 80$ GeV	0.744	0.691	7.2%	0.724	0.677	6.4%
9	At most one jet	0.973	0.979	0.7%	0.972	0.980	0.8%

Table 1.2: Same as in Table 1.1 but for a mediator mass of 200 GeV.

	Selection step	Electron channel			Muon channel		
		$\epsilon_i^{\rm CMS}$	$\epsilon_i^{\rm MA5}$	$\delta_i^{\rm rel}$	$\epsilon_i^{\rm CMS}$	$\epsilon_i^{\rm MA5}$	$\delta_i^{\rm rel}$
1	Two leptons	-	-	-	-	-	-
2	$m_{\ell\ell} \in [80, 100]$ GeV	0.929	0.932	0.4%	0.920	0.929	1.0%
3	$p_T^{\ell\ell} > 50$ GeV	0.676	0.683	1.0%	0.658	0.674	2.5%
4	Third lepton and tau veto	0.959	0.991	3.4%	0.959	0.992	3.5%
5	b-jet veto	0.983	0.931	5.4%	0.984	0.930	5.5%
6	$\left\|\Delta\varphi(\not{\mathbf{p}}_T, \mathbf{p}^{\ell\ell})\right\| > 2.7$	0.703	0.771	9.7%	0.708	0.765	8.1%
7	$\left\|\not{E}_T - p_T^{\ell\ell}\right\|/p_T^{\ell\ell} < 0.2$	0.625	0.724	16.0%	0.641	0.706	10.0%
8	$\not{E}_T > 80$ GeV	0.735	0.714	2.8%	0.745	0.711	4.6%
9	At most one jet	0.979	0.977	0.4%	0.982	0.978	0.2%

Table 1.3: Same as in Table 1.1 but for a mediator mass of 500 GeV.

	Selection step	Electron channel			Muon channel		
		$\epsilon_i^{\rm CMS}$	$\epsilon_i^{\rm MA5}$	$\delta_i^{\rm rel}$	$\epsilon_i^{\rm CMS}$	$\epsilon_i^{\rm MA5}$	$\delta_i^{\rm rel}$
1	Two leptons	-	-	-	-	-	-
2	$m_{\ell\ell} \in [80, 100]$ GeV	0.929	0.931	0.2%	0.922	0.930	0.9%
3	$p_T^{\ell\ell} > 50$ GeV	0.783	0.775	1.0%	0.770	0.765	0.6%
4	Third lepton and tau veto	0.953	0.990	3.9%	0.952	0.990	4.0%
5	b-jet veto	0.980	0.918	6.3%	0.982	0.918	6.5%
6	$\left\|\Delta\varphi(\not{\mathbf{p}}_T, \mathbf{p}^{\ell\ell})\right\| > 2.7$	0.719	0.770	7.2%	0.718	0.767	6.8%
7	$\left\|\not{E}_T - p_T^{\ell\ell}\right\|/p_T^{\ell\ell} < 0.2$	0.672	0.726	8.0%	0.662	0.718	8.4%
8	$\not{E}_T > 80$ GeV	0.860	0.819	4.7%	0.854	0.809	5.3%
9	At most one jet	0.954	0.966	1.3%	0.956	0.972	1.7%

Table 1.4: Same as in Table 1.1 but for a mediator mass of 1000 GeV.

	Selection step	Electron channel			Muon channel		
		$\epsilon_i^{\rm CMS}$	$\epsilon_i^{\rm MA5}$	$\delta_i^{\rm rel}$	$\epsilon_i^{\rm CMS}$	$\epsilon_i^{\rm MA5}$	$\delta_i^{\rm rel}$
1	Two leptons	-	-	-	-	-	-
2	$m_{\ell\ell} \in [80, 100]$ GeV	0.928	0.931	0.4%	0.921	0.927	0.7%
3	$p_T^{\ell\ell} > 50$ GeV	0.835	0.822	1.6%	0.825	0.807	2.2%
4	Third lepton and tau veto	0.948	0.988	4.2%	0.949	0.990	4.3%
5	b-jet veto	0.977	0.904	7.5%	0.979	0.903	7.7%
6	$\left\lvert\Delta\varphi(\not{\mathbf{p}}_T, \mathbf{p}^{\ell\ell})\right\rvert > 2.7$	0.705	0.766	8.6%	0.695	0.759	9.1%
7	$\left\lvert\not{E}_T - p_T^{\ell\ell}\right\rvert / p_T^{\ell\ell} < 0.2$	0.678	0.725	6.9%	0.668	0.708	5.9%
8	$\not{E}_T > 80$ GeV	0.915	0.870	4.9%	0.902	0.863	4.3%
9	At most one jet	0.936	0.960	2.5%	0.943	0.961	1.9%

Table 1.5: Same as in Table 1.1 but for a mediator mass of 5000 GeV.

	Selection step	Electron channel			Muon channel		
		$\epsilon_i^{\rm CMS}$	$\epsilon_i^{\rm MA5}$	$\delta_i^{\rm rel}$	$\epsilon_i^{\rm CMS}$	$\epsilon_i^{\rm MA5}$	$\delta_i^{\rm rel}$
1	Two leptons	-	-	-	-	-	-
2	$m_{\ell\ell} \in [80, 100]$ GeV	0.928	0.931	0.3%	0.921	0.928	0.7%
3	$p_T^{\ell\ell} > 50$ GeV	0.841	0.839	0.2%	0.832	0.827	0.6%
4	Third lepton and tau veto	0.947	0.988	4.3%	0.945	0.988	4.6%
5	b-jet veto	0.977	0.893	8.6%	0.978	0.894	8.6%
6	$\left\lvert\Delta\varphi(\not{\mathbf{p}}_T, \mathbf{p}^{\ell\ell})\right\rvert > 2.7$	0.708	0.760	7.3%	0.698	0.754	8.0%
7	$\left\lvert\not{E}_T - p_T^{\ell\ell}\right\rvert / p_T^{\ell\ell} < 0.2$	0.687	0.720	4.9%	0.684	0.703	2.7%
8	$\not{E}_T > 80$ GeV	0.923	0.889	3.7%	0.908	0.879	3.2%
9	At most one jet	0.932	0.953	2.2%	0.935	0.954	2.1%

At each step of the validation, the MADANALYSIS 5 predictions and the official CMS results have been found to agree at a level of about 10% or below, with the exception of the selection on the momentum balance of the event for scenarios where the mediator mass is small (10 GeV or 200 GeV). In this case, the CMS results are only described at the level of 10%–15% by MADANALYSIS 5. This discrepancy can be traced back to the fast simulation of the detector by DELPHES for which a proper description of the missing energy is harder to achieve. The latter indeed depends on all the other objects in the events and is thus sensitive to all the aspect of the detector simulation.

In Table 1.6, we calculate the total efficiency of the analysis for both signal regions and confront the results obtained in the MADANALYSIS 5 framework with the official ones provided by the CMS collaboration. The efficiencies are defined as

$$\epsilon = \frac{n_9}{n_1} \,, \tag{1.7}$$

where n_1 and n_9 are the number of events that are selected after the first cut (i.e.,, the selection on the number of signal leptons) and the number of events surviving all cuts, respectively. The difference between MADANALYSIS 5 and CMS is evaluated again relatively to the CMS results,

$$\delta^{\rm rel} = \left| 1 - \frac{\epsilon^{\rm MA5}}{\epsilon^{\rm CMS}} \right| . \tag{1.8}$$

Table 1.6: Comparison of the selection efficiencies obtained with our MADANALYSIS 5 reimplementation (MA5) to those provided by the CMS collaboration (CMS) for a dark matter benchmark scenario where the dark matter mass has been set to 50 GeV and the mediator mass $m_{Z'}$ is varying. All vector couplings of the mediator have been fixed to 1. The results are expressed in terms of the total selection efficiency as defined in Eq. (1.7), and the relative difference $\delta^{\rm rel}$ between the CMS and the MADANALYSIS 5 efficiencies is computed as in Eq. (1.8).

Scenario	Electron channel			Muon channel		
	$\epsilon^{\rm CMS}$	$\epsilon^{\rm MA5}$	$\delta^{\rm rel}$	$\epsilon^{\rm CMS}$	$\epsilon^{\rm MA5}$	$\delta^{\rm rel}$
$m_{Z'} = 10$ GeV	0.178	0.219	16.0%	0.173	0.200	13.0%
$m_{Z'} = 200$ GeV	0.186	0.230	23.0%	0.189	0.220	15.0%
$m_{Z'} = 500$ GeV	0.269	0.291	8.0%	0.258	0.280	8.6%
$m_{Z'} = 1000$ GeV	0.294	0.320	7.9%	0.279	0.300	6.8%
$m_{Z'} = 5000$ GeV	0.302	0.320	5.7%	0.287	0.300	4.8%

An agreement at the level of 10%–20% has been found, resulting from the cumulative effect of all the cuts, the agreement being once again better for the heavy mediator case.

In Figure 1.2, we compare normalized missing transverse energy distributions at different level of the analysis. Results for the electron and muon channels are presented in the left and right panel of the figure, respectively, and are given for the benchmark scenario in which the mediator mass has been set to 200 GeV.

In the upper panel of the figure, all the preselection cuts (i.e.,, the first five cuts) have been applied, together with the requirement that at most one jet is present in the selected events (i.e.,, the last of all cuts). This change in the cut ordering is necessary to map what has been done by CMS to produce the validation material. In the lower panel of the figure, we show the same distributions but after imposing all selection cuts. We observe a fair agreement between the MADANALYSIS 5 predictions and the official numbers, the shapes of the distributions qualitatively matching well. The peaking bins are indeed in accordance with the official results and the differences for the higher-missing energy bins are of at most 10%-15%. This level of accuracy is similar to what has been found for the cutflow in Table 1.2. We also observe that the largest difference of 23% and 15% obtained for the total efficiencies in the electron and muon signal region, respectively, is due to the impact of the tail of the missing energy distributions.

Analyzing the previous results, the differences between the theory predictions and the finding of CMS seem to push towards a mismodeling of the missing energy. The latter is known to be very sensitive to pileup effects, so that we perform the exercise a second time, using instead a DELPHES cards including the modeling of the pileup. The results are shown in Table 1.7, Table 1.8, Table 1.9, Table 1.10 and Table 1.11 for the cutflows associated with the different signals under consideration, as well as in Table 1.12 for the total signal efficiency. Distributions in the missing energy for the two signal regions are given in Figure 1.3. We observe a much better agreement at all levels.

This leads us to the conclusion that the implementation of the CMS-EXO-16-010 analysis within the MADANALYSIS 5 framework can be considered as validated. We have found a level of agreement with the experimental results that is of 5–10%, so that any prediction that would be made with the MADANALYSIS 5 framework could be seen as reasonably accurate. The DELPHES parameterization including the pileup effects is the one that is recommended to be used.

The DOI that has been assigned to the CMS-EXO-16-010 MADANALYSIS 5 reimplementation is given by

`10.7484/INSPIREHEP.DATA.RK53.S39D`

Table 1.7: Same as in Table 1.1 but when the pileup modeling is included in the MADANALYSIS 5 recasting.

	Selection step	Electron channel			Muon channel		
		$\epsilon_i^{\rm CMS}$	$\epsilon_i^{\rm MA5}$	$\delta_i^{\rm rel}$	$\epsilon_i^{\rm CMS}$	$\epsilon_i^{\rm MA5}$	$\delta_i^{\rm rel}$
1	Two leptons	-	-	-	-	-	-
2	$m_{\ell\ell} \in [80, 100]$ GeV	0.929	0.931	0.2%	0.919	0.929	1.1%
3	$p_T^{\ell\ell} > 50$ GeV	0.647	0.651	0.7%	0.644	0.637	1.1%
4	Third lepton and tau veto	0.963	0.989	2.7%	0.961	0.989	2.9%
5	b-jet veto	0.983	0.933	5.1%	0.984	0.935	5.0%
6	$\left\vert\Delta\varphi(\not{\mathbf{p}}_T, \mathbf{p}^{\ell\ell})\right\vert > 2.7$	0.694	0.700	0.9%	0.705	0.699	0.9%
7	$\left\vert\not{E}_T - p_T^{\ell\ell}\right\vert / p_T^{\ell\ell} < 0.2$	0.623	0.585	6.1%	0.623	0.577	7.3%
8	$\not{E}_T > 80$ GeV	0.744	0.760	2.2%	0.724	0.744	2.8%
9	At most one jet	0.973	0.965	0.7%	0.972	0.973	0.1%

Table 1.8: Same as in Table 1.2 but when the pileup modeling is included in the MADANALYSIS 5 recasting.

	Selection step	Electron channel			Muon channel		
		$\epsilon_i^{\rm CMS}$	$\epsilon_i^{\rm MA5}$	$\delta_i^{\rm rel}$	$\epsilon_i^{\rm CMS}$	$\epsilon_i^{\rm MA5}$	$\delta_i^{\rm rel}$
1	Two leptons	-	-	-	-	-	-
2	$m_{\ell\ell} \in [80, 100]$ GeV	0.929	0.930	0.1%	0.920	0.927	0.7%
3	$p_T^{\ell\ell} > 50$ GeV	0.676	0.680	0.6%	0.658	0.675	2.7%
4	Third lepton and tau veto	0.959	0.987	3.0%	0.959	0.989	3.1%
5	b-jet veto	0.983	0.934	5.0%	0.984	0.930	5.5%
6	$\left\vert\Delta\varphi(\not{\mathbf{p}}_T, \mathbf{p}^{\ell\ell})\right\vert > 2.7$	0.703	0.705	0.3%	0.708	0.707	0.1%
7	$\left\vert\not{E}_T - p_T^{\ell\ell}\right\vert / p_T^{\ell\ell} < 0.2$	0.625	0.599	4.1%	0.641	0.585	8.7%
8	$\not{E}_T > 80$ GeV	0.735	0.781	6.4%	0.745	0.777	4.2%
9	At most one jet	0.979	0.963	1.1%	0.982	0.962	1.7%

Table 1.9: Same as in Table 1.3 but when the pileup modeling is included in the MADANALYSIS 5 recasting.

	Selection step	Electron channel			Muon channel		
		$\epsilon_i^{\rm CMS}$	$\epsilon_i^{\rm MA5}$	$\delta_i^{\rm rel}$	$\epsilon_i^{\rm CMS}$	$\epsilon_i^{\rm MA5}$	$\delta_i^{\rm rel}$
1	Two leptons	-	-	-	-	-	-
2	$m_{\ell\ell} \in [80, 100]$ GeV	0.929	0.929	0.0%	0.922	0.927	0.5%
3	$p_T^{\ell\ell} > 50$ GeV	0.783	0.777	0.7%	0.770	0.765	0.7%
4	Third lepton and tau veto	0.953	0.987	3.6%	0.952	0.987	3.7%
5	b-jet veto	0.980	0.919	6.2%	0.982	0.922	6.1%
6	$\left\vert\Delta\varphi(\not{\mathbf{p}}_T, \mathbf{p}^{\ell\ell})\right\vert > 2.7$	0.719	0.726	1.1%	0.718	0.726	1.0%
7	$\left\vert\not{E}_T - p_T^{\ell\ell}\right\vert / p_T^{\ell\ell} < 0.2$	0.672	0.634	5.7%	0.662	0.622	6.2%
8	$\not{E}_T > 80$ GeV	0.860	0.872	1.4%	0.854	0.861	0.8%
9	At most one jet	0.954	0.952	0.2%	0.956	0.954	0.2%

Table 1.10: Same as in Table 1.4 but when the pileup modeling is included in the MADANALYSIS 5 recasting.

	Selection step	Electron channel			Muon channel		
		$\epsilon_i^{\rm CMS}$	$\epsilon_i^{\rm MA5}$	$\delta_i^{\rm rel}$	$\epsilon_i^{\rm CMS}$	$\epsilon_i^{\rm MA5}$	$\delta_i^{\rm rel}$
1	Two leptons	-	-	-	-	-	-
2	$m_{\ell\ell} \in [80, 100]$ GeV	0.928	0.929	0.2%	0.921	0.925	0.4%
3	$p_T^{\ell\ell} > 50$ GeV	0.835	0.824	1.4%	0.825	0.810	1.8%
4	Third lepton and tau veto	0.948	0.985	3.9%	0.949	0.986	4.0%
5	b-jet veto	0.977	0.908	7.1%	0.979	0.910	7.1%
6	$\left\|\Delta\varphi(\not{\mathbf{p}}_T, \mathbf{p}^{\ell\ell})\right\| > 2.7$	0.705	0.733	4.0%	0.695	0.730	4.9%
7	$\left\|\not{E}_T - p_T^{\ell\ell}\right\|/p_T^{\ell\ell} < 0.2$	0.678	0.648	4.4%	0.668	0.631	5.5%
8	$\not{E}_T > 80$ GeV	0.915	0.910	0.6%	0.902	0.899	0.4%
9	At most one jet	0.936	0.940	0.4%	0.943	0.941	0.2%

Table 1.11: Same as in Table 1.5 but when the pileup modeling is included in the MADANALYSIS 5 recasting.

	Selection step	Electron channel			Muon channel		
		$\epsilon_i^{\rm CMS}$	$\epsilon_i^{\rm MA5}$	$\delta_i^{\rm rel}$	$\epsilon_i^{\rm CMS}$	$\epsilon_i^{\rm MA5}$	$\delta_i^{\rm rel}$
1	Two leptons	-	-	-	-	-	-
2	$m_{\ell\ell} \in [80, 100]$ GeV	0.928	0.931	0.1%	0.921	0.923	0.3%
3	$p_T^{\ell\ell} > 50$ GeV	0.841	0.844	0.4%	0.832	0.833	0.2%
4	Third lepton and tau veto	0.947	0.985	4.0%	0.945	0.986	4.3%
5	b-jet veto	0.977	0.895	8.4%	0.978	0.897	8.3%
6	$\left\|\Delta\varphi(\not{\mathbf{p}}_T, \mathbf{p}^{\ell\ell})\right\| > 2.7$	0.708	0.739	4.4%	0.698	0.728	4.3%
7	$\left\|\not{E}_T - p_T^{\ell\ell}\right\|/p_T^{\ell\ell} < 0.2$	0.687	0.661	3.8%	0.684	0.644	5.9%
8	$\not{E}_T > 80$ GeV	0.923	0.928	0.6%	0.908	0.018	1.1%
9	At most one jet	0.932	0.926	0.7%	0.935	0.930	0.5%

Table 1.12: Same as in Table 1.6 when the pileup modeling is included in the MADANALYSIS 5 recasting.

Scenario	Electron channel			Muon channel		
	$\epsilon^{\rm CMS}$	$\epsilon^{\rm MA5}$	$\delta^{\rm rel}$	$\epsilon^{\rm CMS}$	$\epsilon^{\rm MA5}$	$\delta^{\rm rel}$
$m_{Z'} = 10$ GeV	0.178	0.170	5.5%	0.173	0.160	7.6%
$m_{Z'} = 200$ GeV	0.186	0.186	0.3%	0.189	0.180	5.8%
$m_{Z'} = 500$ GeV	0.269	0.250	6.9%	0.258	0.240	7.3%
$m_{Z'} = 1000$ GeV	0.294	0.280	5.4%	0.279	0.260	6.1%
$m_{Z'} = 5000$ GeV	0.302	0.290	4.3%	0.287	0.270	5.1%

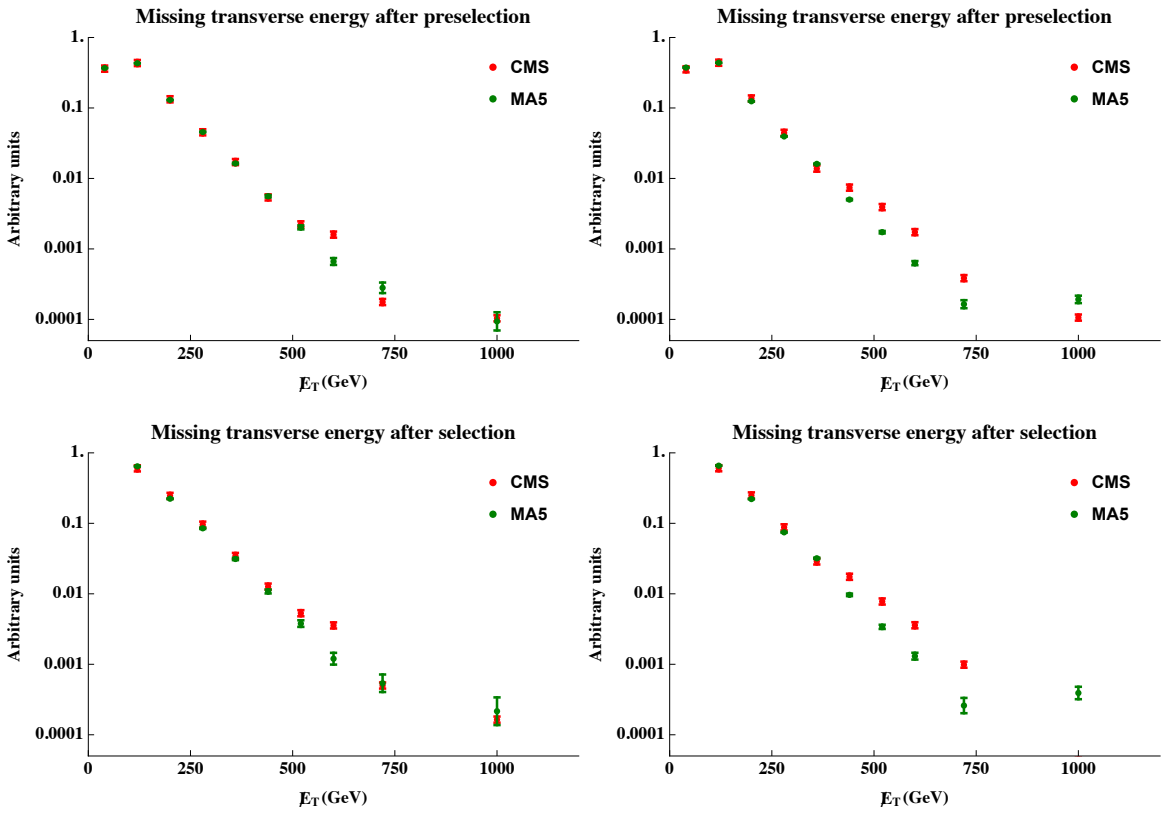

Fig. 1.2: Missing transverse energy spectrum in the electron channel (left) and in the muon channel (right) after all preselection cuts including the requirement on the number of jets (upper panel) and after all cuts (lower panel). We compare the official CMS results (red) including a 10% Monte Carlo uncertainty with the results obtained with MADANALYSIS 5 (green), the statistical uncertainties being included for the latter.

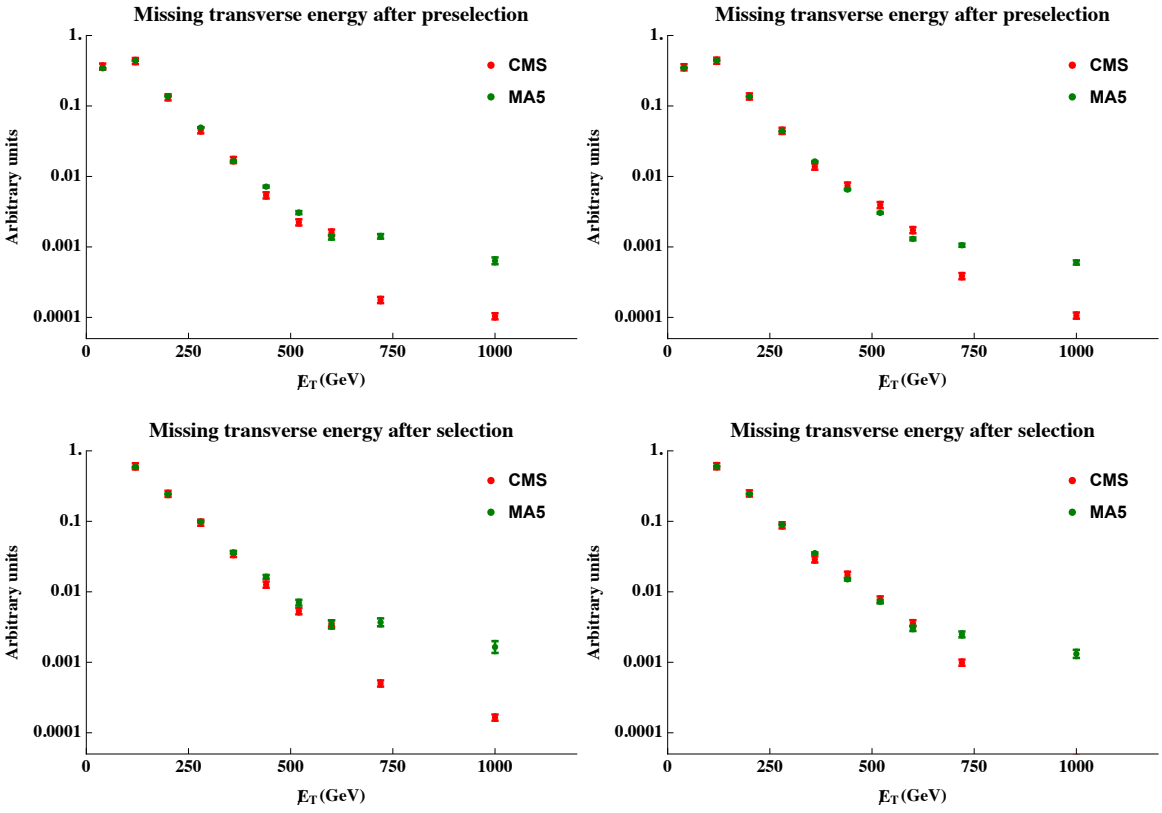

Fig. 1.3: Same as in Figure 1.2 but when the pileup modeling is included in the MADANALYSIS 5 recasting.

References

[1] D. Abercrombie et al., *Dark Matter Benchmark Models for Early LHC Run-2 Searches: Report of the ATLAS/CMS Dark Matter Forum*, arXiv:1507.00966. 5

[2] H. Georgi, *Unparticle Physics*, *Phys. Rev. Lett.* **98** (2007) 221601, [hep-ph/0703260]. 5

[3] H. Georgi, *Another Odd Thing About Unparticle Physics*, *Phys. Lett.* **B650** (2007) 275–278, [arXiv:0704.2457]. 5

[4] J. Alwall, R. Frederix, S. Frixione, V. Hirschi, F. Maltoni, O. Mattelaer, H. S. Shao, T. Stelzer, P. Torrielli, and M. Zaro, *The automated computation of tree-level and next-to-leading order differential cross sections, and their matching to parton shower simulations*, *JHEP* **07** (2014) 079, [arXiv:1405.0301]. 6

[5] T. Sjöstrand, S. Ask, J. R. Christiansen, R. Corke, N. Desai, P. Ilten, S. Mrenna, S. Prestel, C. O. Rasmussen, and P. Z. Skands, *An Introduction to PYTHIA 8.2*, *Comput. Phys. Commun.* **191** (2015) 159–177, [arXiv:1410.3012]. 6

[6] P. Skands, S. Carrazza, and J. Rojo, *Tuning PYTHIA 8.1: the Monash 2013 Tune*, *Eur. Phys. J.* **C74** (2014), no. 8 3024, [arXiv:1404.5630]. 6

[7] **NNPDF** Collaboration, R. D. Ball et al., *Parton distributions for the LHC Run II*, *JHEP* **04** (2015) 040, [arXiv:1410.8849]. 6

[8] A. Buckley, J. Ferrando, S. Lloyd, K. Nordström, B. Page, M. Rüfenacht, M. Schönherr, and G. Watt, *LHAPDF6: parton density access in the LHC precision era*, *Eur. Phys. J.* **C75** (2015) 132, [arXiv:1412.7420]. 6

[9] J. Alwall, C. Duhr, B. Fuks, O. Mattelaer, D. G. Öztürk, and C.-H. Shen, *Computing decay rates for new physics theories with FeynRules and MadGraph 5_aMC@NLO*, *Comput. Phys. Commun.* **197** (2015) 312–323, [arXiv:1402.1178]. 6